

10-2006

Interfacial Stick-Slip Transition in Simple Shear of Entangled Melts

Pouyan E. Boukany

University of Akron Main Campus

Prashant Tapadia

University of Akron Main Campus

Shi-Qing Wang

University of Akron Main Campus, swang@uakron.edu

Please take a moment to share how this work helps you [through this survey](#). Your feedback will be important as we plan further development of our repository.

Follow this and additional works at: http://ideaexchange.uakron.edu/polymer_ideas



Part of the [Polymer Science Commons](#)

Recommended Citation

Boukany, Pouyan E.; Tapadia, Prashant; and Wang, Shi-Qing, "Interfacial Stick-Slip Transition in Simple Shear of Entangled Melts" (2006). *College of Polymer Science and Polymer Engineering*. 97.

http://ideaexchange.uakron.edu/polymer_ideas/97

This Article is brought to you for free and open access by IdeaExchange@UAkron, the institutional repository of The University of Akron in Akron, Ohio, USA. It has been accepted for inclusion in College of Polymer Science and Polymer Engineering by an authorized administrator of IdeaExchange@UAkron. For more information, please contact mjon@uakron.edu, uapress@uakron.edu.

Interfacial stick-slip transition in simple shear of entangled melts

Pouyan E. Boukany, Prashant Tapadia, and Shi-Qing Wang^{a)}

Department of Polymer Science, University of Akron, Akron, Ohio 44325

(Received 5 December 2005; final revision received 23 June 2006)

Synopsis

This article describes a systematic investigation of a discontinuous interfacial stick-slip transition (SST) in *simple shear* of monodisperse entangled 1,4-polybutadiene (PBD) and polyisoprene (PIP) melts with different molecular weights and architecture, using a specially designed controlled-force shear rheometer. The magnitude of the transition is found to be determined by the level of chain entanglement. Specifically, the dependence of extrapolation length b on molecular weight as $b \sim M_w^{3.4}$ and of the melt viscosity as $b \sim \eta$ is consistent with the observations based on capillary rheometric studies [X. Yang *et al.*, *Rheol. Acta* **37**, 415–423 (1998)]. The interfacial nature of the flow behavior is explicitly demonstrated by a surface treatment of the shearing plates and dependence of the abrupt increase of the apparent shear rate on the gap distance as well as by particle tracking velocimetry. The critical stress for different molecular weights of PBD and PIP is about 0.2 and 0.1 MPa, respectively, independent of molecular weight and architecture. These results are consistent with the previous conclusion of an interfacial SST as the origin of the discontinuous spurt flow behavior observed with pressure-driven capillary rheometry. The critical stress for the SST is found to be lower in simple shear flow. Finally, chain architecture is observed to also influence the magnitude of the SST apart from the level of chain entanglement. © 2006 *The Society of Rheology*. [DOI: 10.1122/1.2241989]

I. INTRODUCTION

Hydrodynamic boundary condition (HBC) plays a crucial role in the characterization of flow behavior of various fluids. Since the time of Navier and Stokes, the postulate of no-slip or stick HBC has been brought into question [Navier (1823); Stokes (1845)]. For polymeric liquids, the first piece of evidence for slip of a macroscopic magnitude appears to be a capillary-flow rheometric study of high-density polyethylene (HDPE) by Bagley and co-workers (1958). This important phenomenon of interfacial origin was later suggested by Vinogradov (1972), Doi and Edwards (1979), McLeish and Ball (1986) to reflect bulk flow behavior of entangled polymers. The “paradox” [Denn (1990)] has since been resolved to our satisfaction. There is no extensive parallel work to illustrate polymer melt flow behavior in simple shear under constant force. A first study involving a force-controlled shear device was published by Laun (1982) who reported a stick-slip like transition in HDPE in a sandwich rheometer.

More recent experimental studies of polymer slip in simple shear from three groups have been based on a sliding plate device [Migler *et al.* (1993); Leger (2003); Mhetar and

^{a)} Author to whom correspondence should be addressed; electronic mail: swang@uakron.edu

Archer (1998a, 1998b); Dao and Archer (2002); Koran and Dealy (1999)] that operates in the mode of an imposed velocity on one of the two parallel plates. By directly determining the melt velocity within 70 nm from the wall using a rather sophisticated method, Leger and co-workers [Durliat *et al.* (1997); Massey *et al.* (1998)] were able to reveal a *smooth* transition from weak slip to strong slip by plotting the slip velocity V_s against the imposed wall velocity (no information on shear stress was collected in these studies), where one can actually infer that the onset stress σ_c for strong slip is essentially independent of the melt molecular weight. However, no scaling behavior of the slip length b_∞ in the strong slip regime was described. On other hand, by carrying out straightforward particle tracking velocimetric observations, it was shown that V_s jumped sharply as a function of the measured shear stress, a signature of transition from weak to strong slip [Mhetar and Archer (1998a, 1998b)]. However, depending on the melt molecular weight and surface condition, a flow (i.e., stick-slip) instability could take place upon reaching the strong slip regime, where it is problematic to define a single slip length b . In a subsequent paper, Dao and Archer (2002) also showed that in the strong slip regime the measured shear stress fluctuated in time, making it difficult to verify the scaling of $b \sim M_w^{3,4}$ [Yang *et al.* (1998)] for a discontinuous interfacial stick-slip transition observed in capillary rheometry. This stress oscillation was also observed by Leger (2003). For the weak slip behavior, Dao and Archer (2002) used the gap dependence of the stress versus shear rate curve to compute the slip length b as a function of the molecular weight. The scaling with the polymer molecular weight was found to be nonuniversal. Koran and Dealy (1999) performed a similar Mooney-type analysis to infer the slip behavior and found a smooth change of V_s with the measured stress.

Since b is always found to be a constant independent of the imposed surface velocity in the weak slip regime [Durliat *et al.* (1997); Massey *et al.* (1998)], it is indeed equivalent to shear the sample in a sliding plate device using either an imposed surface velocity or a constant surface force. However, the stick-slip instability observed in the imposed velocity mode clearly indicates the disadvantage of adopting such a mode for studying the strong slip behavior. Fundamentally, it is the shear stress—exerted on the surface-tethered interfacial chains—that determines the state of the entanglement and disentanglement with the bulk chains. Imposing a constant surface velocity does not ensure that the surface shear stress could be held constant during an experiment designed to probe the strong slip regime, and may often lead to stick-slip instability as observed by Dao and Archer (2003) and Leger (2003).

For the reasons indicated in the preceding paragraph, to characterize the strong slip regime, there is a need to build a sliding plate device where the shearing force is the controlled variable. The motivation for this work also stems from a recent question about the nature of spurt flow in capillary rheometry. There has been a suggestion in the literature [Smillo (2004)] that the origin of the previously reported interfacial slip-stick transition (SST) in capillary flow might be a system instability, related to the design of the controlled-pressure capillary rheometer. Do entangled polymers really undergo a *discontinuous* interfacial SST in viscometric flow? Since it is the interfacial shear stress that determines the nature of the HBC for entangled polymers on solid surfaces, this question should be answered by employing a shearing device where the wall stress is controlled.

The purpose of this work is to find out, through design and application of a force-controlled sliding co-cylinder rheometer, whether a *discontinuous* interfacial SST would take place in simple shear flow where the shear stress is approximately uniform across the gap. Using this simple device, we bypass any complications associated with a pressure-controlled capillary rheometer. We carry out this investigation based on linear 1,4-

TABLE I. Molecular characteristics of PBDs.

Sample	T_g (°C)	1-2PBD	1,4-PBD	M_n (kg/mol)	M_w (kg/mol)	M_w/M_n	Source
100 K	-100.1	8.2	91.8	98.85	99.06	1.002	Goodyear
207 K	-100.5	8.1	91.9	207.3	207.7	1.002	Goodyear
400 K	-99.5	7.7	92.3	410.8	411.5	1.004	Goodyear
740 K	-99.5	10	90	740	750	1.07	Bridgestone
Four-arm star (400 K)	-99.5	10	90	411.2	430.5	1.107	Goodyear

polybutadiene (PBD) of various molecular weights, a four-arm star of 1,4-PBD, and linear 1,4-polyisoprene (PIP) of various molecular weights.

II. EXPERIMENT

A. Materials

The materials under investigation are a series of high molecular weight monodisperse PBD and PIP of different molecular weights. The main characteristics of these samples are listed in Tables I and II. All samples were made in Adel Halasa's Lab at Goodyear, except for the 740 K PBD that we gratefully received from Chris Robertson at Bridgestone America.

B. Apparatus

1. Commercial capillary rheometer

A pressure-controlled Monsanto automatic capillary rheometer (MACR) is employed to provide capillary rheometric characterization of the SST phenomenon, as well as a benchmark for the home-made piston-shear rheometer described below. The nominal wall shear rate $\dot{\gamma}$ is calculated according to $\dot{\gamma} = 32Q/\pi D^3$, without the Rabinowitsch correction; and the nominal wall shear stress σ is computed from the applied pressure P according to $\sigma = (D/4L)P$, without the Bagley correction. For the slow-flowing high molecular weight samples, the flow rate Q is estimated by collecting and weighing the extrudate: $Q = M/\rho t$, where M is the weight of the extrudate, ρ is the density of the extrudate (0.9 g/cm³), and t is the time of extrusion. All measurements were carried out at room temperature around 25 °C.

TABLE II. Molecular characteristics of PIPs.

Polymer ID	T_g (°C)	Microstructure (%)			Molecular weight (GPC)			Source
		Cis-1,4	Trans- 1,4	3,4-	M_n	M_w	M_w/M_n	
11272-39-4	-65	75.0	18.4	6.6	180 K	190 K	1.06	Goodyear
11272-39-5	-65	75.2	17.8	7.0	291 K	311 K	1.07	Goodyear

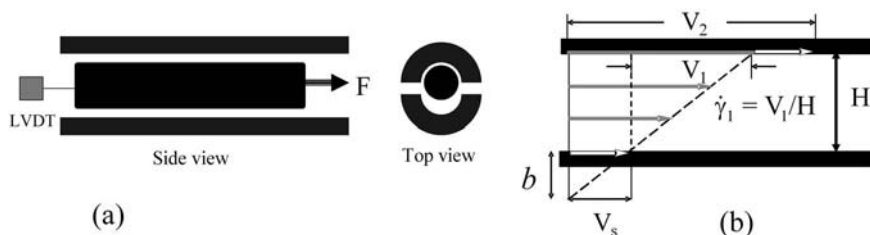


FIG. 1. (a) Schematic depiction of the home-made CFPSR in the configuration of co-cylinders, where the inner cylinder is pulled with a constant force, its speed is measured with a standard LVDT, and the outer cylinder is made of two semicylinders that are closed once the sample has been wrapped around the inner cylinder. (b) Illustration of presence of wall slip upon the SST when the upper plate (corresponding to the inner cylinder) increases its velocity from V_1 to V_2 without any increase in the internal rate of shear $\dot{\gamma}_1$. The slip correction is most conveniently quantified by using the extrapolation length b , as depicted.

2. Home-made simple-shear rheometer

A custom made constant-force piston-shear rheometer (CFPSR) was employed [Segel (1903); Pochettino (1914); Dealy and Giacomin (1988)] developed in our lab to allow rheometric studies of polymer melts in simple shear. It consists of two stainless-steel concentric cylinders as the two shearing surfaces. As illustrated in Fig. 1(a), the inner cylinder is made to move with a prescribed force from an air cylinder (10.9 N FESTO Co.), and its velocity V is determined with a linear voltage differential transformer (LVDT) device (Schaevitz Sensors Co.). The outer cylinder, made of two semicylinders for easy sample loading, has a diameter of 20.21 mm. The device is equipped with inner cylinders of three diameters to provide three gap distances of $H = 0.1, 0.2,$ and 0.4 mm, respectively. The mutual alignment of the two cylinders is achieved by having the inner cylinder fixed in the center of the two-piece outer cylinder, and a uniform layer of sample wrapped around the inner cylinder. Good gap control can be achieved by opening up the outer cylinder several times to trim off the excess sample that flowed into the gaps of the two semicylinders. As a calibration, this rheometer was found to produce identical flow curves for the monodisperse melts in the Newtonian region when compared with results from MACR.

For this apparatus to provide quantitatively reliable rheological data, we often need to estimate the gap distance H between the co-cylinders instead of using the prescribed values of H . The shear stress is calculated according to the total force F exerted on the piston, i.e., on the surface area A of the sample, as $\sigma = F/A$. The weight W of the sample is premeasured so that its volume is first determined as $\Omega = W/\rho$. The gap distance is estimated as $H = \Omega/A = \Omega\sigma/F$. On the Newtonian branch, we know the sample viscosity η from both dynamic shear measurements and capillary rheometry, which is related to shear stress σ as $\eta = \sigma H/V$, where V/H is the shear rate. Thus, by the readings of F and V and knowing Ω and η , we have

$$H = (\Omega \eta V / F)^{1/2}, \quad (1)$$

which can be directly computed for any given loading. Typically, the actual gap distance determined from Eq. (1) is larger than the preset value, by anywhere between 0 and 15%.

To conclude this subsection on the CFPSR, we briefly describe the consequence of an interfacial SST in terms of the measured V of the piston. As illustrated in Fig. 1(b), the piston velocity is V_1 before the SST and V_2 upon the SST. Thus, the jump in V or in the apparent shear rate V/H at the SST is given by

$$V_2/V_1 \equiv \dot{\gamma}_2/\dot{\gamma}_1 = 1 + 2b/H, \quad (2)$$

where the Navier-de Gennes extrapolation length b has the geometric meaning and definition as shown in Fig. 1(b), and is related to the slip velocity V_s as $b = V_s/(V_1/H)$.

3. Sample loading

Bubble-free films of the samples were prepared by solution casting and pressing with CRAVER to produce uniform thickness. A sample with a sufficient length L and thickness H , typically with $L=3$ cm and $H=0.025$ cm, and an aspect ratio $L/H=150$, was placed on the inner piston. Then, the two semiouter cylinders were closed onto each other, squeezing the sample in between the gap. The sample essentially flowed in the axial direction, however, some material can creep into the joint of the two semicylinders. The procedure is then to open up the outer semicylinders to clear the joint and close it again so that the actual gap would not deviate significantly from the preset value of the gap distance H . All measurements were carried out at room temperature, around 25 °C.

4. Surface treatment

To explore whether the flow behavior depends on the surface condition, we can also coat the inner piston with a polysiloxane elastomer to minimize polymer adsorption. Following a previously established procedure [Yang *et al.* (1998)], the coating could be accomplished by injecting a 15 wt % isopropyl acetate solution of copolymer of siloxane (Permalon# M-15, Russell Products Co., Inc.) onto the preheated piston surface and then allowing it to cure at 180 °C for 1 h.

III. RESULTS AND DISCUSSION

We have carried out a systematic study of the melt flow behavior in simple shear under the condition of controlled shearing force. Several important effects have been explored, including the molecular weight dependence of the flow characteristics and the role of chain architecture. The experiments represent our efforts to subject the entangled melts to a constant shearing force, in contrast to previous studies [Koran and Dealy (1999); Dao and Archer (2002); Leger (2003)], where a sliding plate shear device only operates in the mode of displacing one of the two surfaces with a constant velocity. Below, we describe these results in different subsections.

A. Molecular weight dependence

Our previous work helped clarify the interfacial origin of the spurt flow phenomenon in capillary flow of entangled polymers [Wang and Drda (1996); Yang *et al.* (1998); Wang (1999)], and also confirmed a simple scaling expression for the magnitude of the interfacial SST. As indicated in Fig. 1(b) and Eq. (2), the discontinuous increase in the apparent shear rate V/H , or velocity V , of the shearing surface over a gap distance of H can be meaningfully described by the Navier-de Gennes extrapolation length b , which is proportional to the bulk shear viscosity η according to

$$b = (\eta/\eta_i)a = (M_w/M_e)^{3.4}a. \quad (3)$$

At SST, the slip layer of thickness comparable to the tube diameter a possesses a viscosity η_i equal to the unentangled melt of entanglement molecular weight M_e . Thus, the second equality of Eq. (3) follows from an empirical relationship of zero-shear viscosity $\eta \sim M_w^{3.4}$ for relatively monodisperse samples. This theoretical prediction [Brochard and de Gennes (1992); Wang (1999)] has been verified by pressure-controlled capillary rhe-

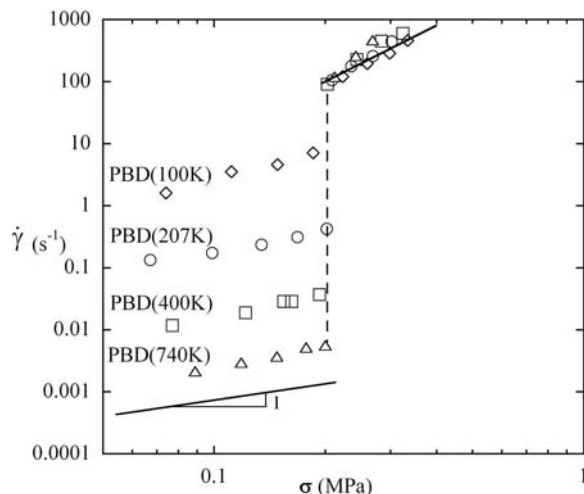


FIG. 2. The nominal shear rate, evaluated according to $\dot{\gamma}=V/H$, as a function of the applied shear stress for four PBD samples of increasing molecular weight (from $M_w=100$ K, 207 K, 410 K to 740 K), where the gap distance H is around 0.23 mm at $T=25$ °C.

ometry in our lab [Wang and Drda (1996); Yang *et al.* (1998)]. This molecular scaling would not hold if there is significant pretransitional wall slip due to less-than-perfect polymer adsorption, nor would it hold for the molecular weight dependence of b calculated from the pretransitional wall slip regime. Finally, under the condition of imposing a velocity V on the shear surface, the values for b are well defined only in the weak slip regime, where no universal molecular weight scaling exists. As a consequence, the previous studies based on strain-controlled sliding plate rheometry [e.g., Dao and Archer (2002)] have not been able to verify the $M_w^{3,4}$ scaling for b involving the SST (strong slip regime).

We further examine the characteristics associated with polymer wall slip by first recognizing that simple shear must be generated with a constant force or shear stress on the wall, so that the shear rate V/H or the plate velocity V is to be a free variable, taking whatever value is determined by the flow response of the melts to the applied force. Using the CFPSR described in Sec. II B 2, we examine the simple shear behavior of highly entangled polymer melts at high stresses. Flow curves shown in Fig. 2 are based on the model melts of linear PBD, showing a SST around $\sigma_c=0.2$ MPa, independent of molecular weight. Note that the previous capillary rheometric study also found σ_c to be M_w independent [Yang *et al.* (1998)]. The magnitude of the SST characterized by b appears to scale linearly with the sample viscosity η and with the molecular weight M_w of the four monodisperse samples as $b \sim M^{3,4}$, which is depicted in Fig. 3, confirming the scaling prediction given in Eq. (3). Moreover, taking the entanglement molecular weight M_e to be 2000 g/mol for PBD and a —as the tube diameter—equal to 4 nm, b is found from Eq. (3) to be on the same order of magnitude as observed experimentally in Fig. 3.

The data in Fig. 2 and capillary flow data in Fig. 1 of Yang *et al.* (1998) both show the overlapping of the upper slip branch for the different molecular weights. This can be easily understood as follows: For these SST of such a large magnitude, $b/H \gg 1$ in Eq. (2), and therefore Eq. (2) becomes

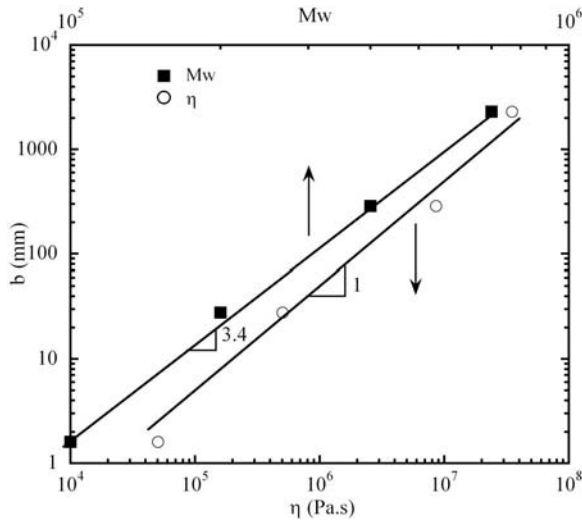


FIG. 3. Extrapolation length b (mm) as a function of the weight average molecular weight M_w and zero-shear viscosity η at $T=25^\circ\text{C}$ for PBD samples.

$$\dot{\gamma}_2 \cong \dot{\gamma}_1(2b/H) = (\sigma_c/\eta)(2\eta/\eta_i)(a/H) = (2\sigma_c/\eta_i)(a/H), \quad (4)$$

which is independent of η , i.e., of M_w , and is determined by the viscosity η_i of the slip layer and layer thickness a for a given H .

The data in Fig. 2 were obtained by applying discrete values of forces on the piston and using the LVDT to measure the displacement of the piston as a function of time. Figure 4 shows the raw data of the displacement for the different applied stresses for the PBD (207 K). At the critical stress, the piston initially moved very slowly; corresponding to flowing on the no-slip branch, until a sufficient amount of strain (just over ten shear

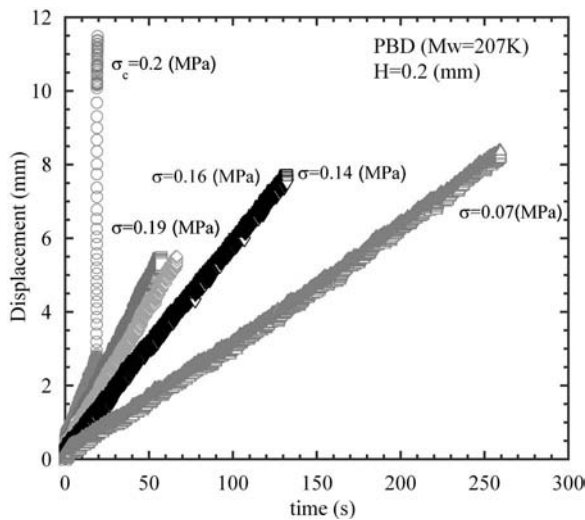


FIG. 4. Displacement of the moving inner piston (mm) as a function of time (s) at different stress levels from 0.07 to 0.2 (MPa) for 207 K PBD, where the gap H is about 0.2 mm at $T=25^\circ\text{C}$.

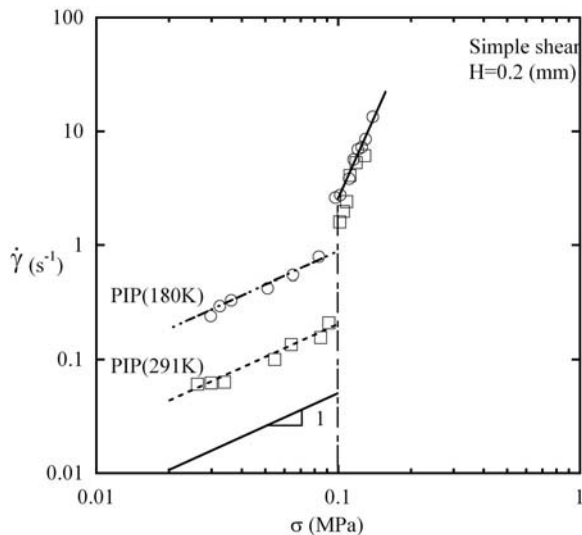


FIG. 5. The nominal shear rate, evaluated according to $\dot{\gamma}=V/H$, as a function of the applied shear stress for two PIP samples of molecular weights 180 K and 291 K, where the gap distance H is around 0.2 mm at $T=25$ °C.

strain units, as shown in Fig. 4) has been experienced by the sample when the piston velocity suddenly jumped substantially (as shown in Fig. 4), confirming a much earlier observation of this feature by Laun (1982). This makes sense because the polymer chains have to suffer sufficient shear deformation before chain disentanglement can take place to cause SST.

The same measurements were carried out for linear PIP samples. As shown in Fig. 5, the SST occurs at a critical stress $\sigma_c=0.1$ MPa. It is important to note that PIP also displays a difference in the onset shear stresses for the SST between parallel-plate simple shear and capillary flow as discussed below.

B. Comparison between CFPSR and pressure-driven capillary rheometry

Before we further elucidate the interfacial nature of the observed SST, we compare the flow curve obtained in simple shear with that from a capillary flow rheometry based on a die with diameter $D=1.0$ mm and aspect ratio $L/D=15$. Figure 6(a) clearly shows that the PBD (207 K) melt underwent an abrupt transition in both planar Couette shear and pressure-driven capillary flow. In other words, the transitional characteristic is not unique to capillary flow. The collapse of data on the lower no-slip flow branch provides a mutual calibration between the two rheometers. More interestingly, the critical stress σ_c for the SST is significantly higher for capillary flow. Since the lower Newtonian branches overlap well for both flow apparatuses, the difference in σ_c must be taken seriously. The same comparison between drag flow and pressure-driven flow was carried out for PIP (291 K). Again the simple-shear apparatus shows a considerably lower σ_c as shown in Fig. 6(b).

It is clear that a high level of hydrostatic pressure P , on the order of $P=(4L/D)\sigma_c=1.2 \times 10^7$ Pa, is present in capillary die flow, and only ambient pressure is present in the simple shear. A majority of the die length feels a hydrostatic pressure of the magnitude of 10^7 Pa. Apparently this hydrostatic pressure postpones the onset of the SST. A comparison with the SST characteristics in a planar Couette shear, as done here, reveals this pressure effect. Since the critical stress σ_c for SST is independent of molecular weight,

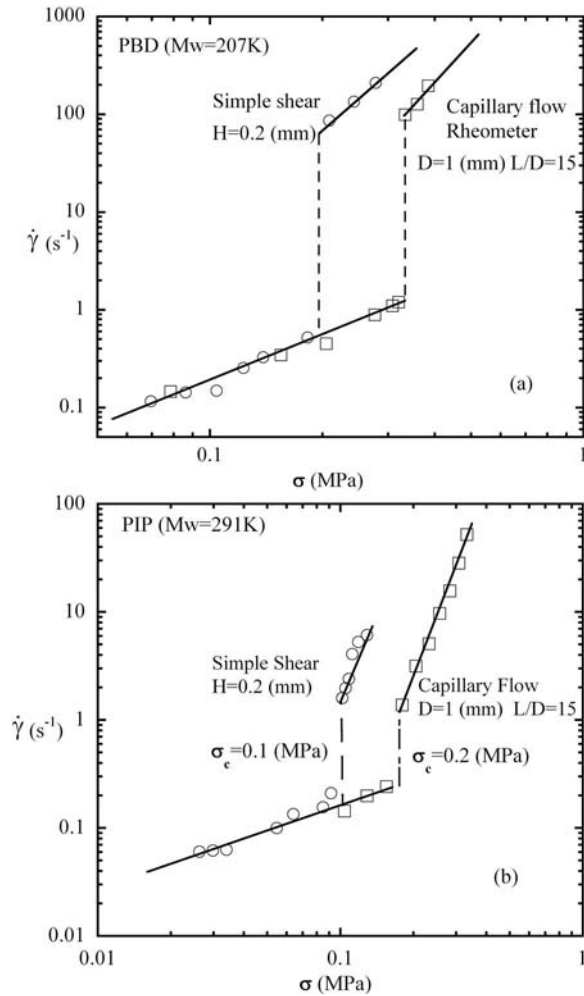


FIG. 6. (a) Comparison of 207 K PBD between flow curves obtained with the present CFPSR and the MACR, where the gap H is around 0.2 mm and capillary die diameter $D=1.0$ mm, with the aspect ratio $L/D=15$ at $T=25$ °C. (b) Comparison of 291 K PIP between flow curves obtained with the present CFPSR and the MACR, where the gap H is around 0.2 mm and capillary die diameter $D=1.0$ mm, with the aspect ratio $L/D=15$ at $T=25$ °C.

full saturation of chain adsorption must have occurred, as observed before [Yang *et al.* (1998)]. However, in the presence of high hydrostatic pressure, chain disentanglement leading to the SST appears to be more difficult.

C. Gap dependence

One of the important characteristics of interfacial wall slip is the gap dependence of the slip correction, as anticipated by Eq. (2). Three different gap distances were employed to determine whether the transition magnitude indeed changes linearly with $1/H$. Figure 7 reveals a clear variation of the jump in the nominal shear rate with the gap distance H . Specifically, the inset in Fig. 7 shows a straight line relating the shear rate ratio to the reciprocal gap distance.

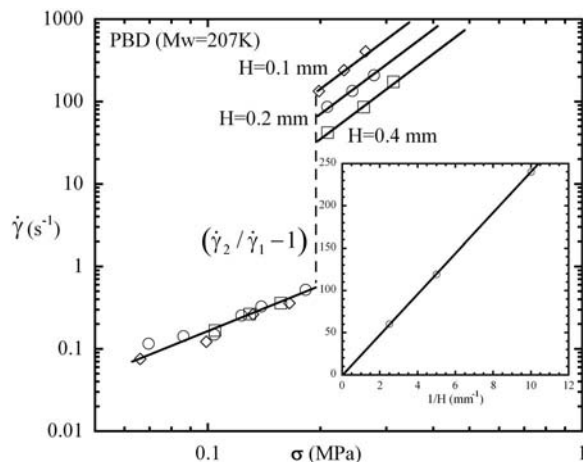


FIG. 7. The discontinuous flow transition examined with three different gap sizes as indicated for 207 K PBD at $T=25$ °C. The inset shows that the abrupt jump in the nominal shear rate as characterized by the ratio $(\dot{\gamma}_2/\dot{\gamma}_1 - 1)$ varies linearly with $1/H$, in agreement with Eq. (2).

D. Effect of surface coating

Since the *discontinuous* flow transition has rarely been seen before in simple shear of entangled melts, we need to look for additional features associated with the transition to firmly establish its physical origin. Specifically, we must directly determine whether the transition is interfacial or constitutive in nature. We coated the inner shearing surface (the piston) with a layer of polysiloxane to make it nonadsorbing. More sophisticated surface treatments have been reported by Leger and co-workers [Durliat *et al.* (1997); Massey *et al.* (1998)]. If the observed flow transition would still take place in the shear cell in spite of the surface coating, then the phenomenon would be constitutive rather than interfacial. Figure 8 shows that the surface coating caused massive wall slip to occur due to stress-induced desorption. Since only one of the two surfaces was coated, the squares in Fig. 8 could not merge with the circles on the upper slip branch until the stick-slip transition also took place on the bare surface of the outer cylinder around 0.2 MPa, as expected from Figs. 2 and 7. It is remarkable that indeed an increase by a factor of ~ 2 is visible at $\sigma=0.2$ MPa in Fig. 8.

E. Effect of chain architecture

The flow behavior of linear and four-arm-star PBD (400 K) is presented in Fig. 9(a). For both star and linear PBD, the SST was observed at the same critical stress $\sigma_c=0.2$ MPa. Thus, σ_c appears to be independent of chain architecture. Being a four-arm star, the no-slip branch is no longer Newtonian, even at 0.1 MPa; having a much higher slope of around 3.0 instead of 1.0. It is surprising to see that the upper slip branches do not converge. This indicates that for different chain architectures the characteristics of the slip layer could be different. The data of the upper branches in Fig. 9(a) would indicate, according to Eq. (4), that the value of (a/η_i) is smaller for the four-arm star PBD than for the linear PBD. It is reassuring to see in Fig. 9(a) that pressure-driven capillary rheometry also confirms the observed difference due to the difference in the chain architectures. It should not come as a total surprise that, for example, the viscosity η_i of the slip layer is

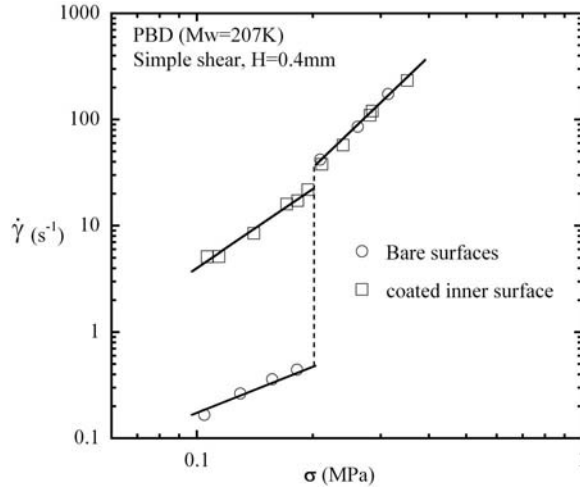


FIG. 8. Coating of the inner cylinder wall with a polysiloxane shows the effect of causing wall slip to occur adhesively throughout the applied stress range, leading to the removal of the SST observed with the bare cylinder surfaces. Here, the gap distance H is 0.4 mm at $T=25^\circ\text{C}$. The remaining small jump (in the squares) around 0.2 MPa results from the SST taking place on the outer bare cylinder wall.

higher for the four-arm star PBD than for the linear PBD, whereas the slip layer thickness, being determined by the tube diameter a , is probably the same for both linear and starlike PBD chains.

For a better understanding of the difference (a/η_i) between the linear and four-arm PBD, the inner piston was coated with polysiloxane. Figure 9(b) shows that the upper slip branch of four-arm star sample with the coated inner piston stays between the linear and star PBD branches obtained with the bare surfaces. Clearly, the coating could restore the value of (a/η_i) only on the coated surface, but a significantly different value of (a/η_i) remains at the interface of the star-PBD and the outer cylinder surface.

In passing, it is interesting to remark that the SST took place at 0.2 MPa for PBD and 0.1 MPa for PIP. Since the elastic plateau modulus G_N^0 of 1,4-PBD and 1,4-PIP is about 1.15 MPa and 0.35 MPa, respectively [Fetters *et al.* (1994)], the polymer chains in the bulk of these monodisperse samples have hardly experienced any significant deformation γ according to $\gamma \sim \sigma_c/G_N^0 = 20\%$ for PBD and 29% for PIP. It appears that the polymer chains in the surface layer must be more effectively oriented to produce disentanglement under conditions where bulk chain disentanglement does not occur. How bulk chains disentangle in polymer melts remains to be elucidated. Our recent and ongoing work on entangled polymer solutions reveals a yieldlike second-order flow transition via bulk chain disentanglement [Tapadia and Wang (2004, 2006)]. The present study clearly indicates that a discontinuous interfacial SST does occur first. Our future work will endeavor to determine whether a constitutive transition would occur in the bulk of entangled polymer melts.

F. Direct determination of velocity field

As a first examination of the actual velocity field change associated with the SST, we combined a customer-made parallel-plate sliding rheometer with a particle-tracking velocimetric (PTV) technique identical to that used recently to study the constitutive shear behavior of entangled polymer solutions [Tapadia and Wang (2006); Tapadia *et al.*

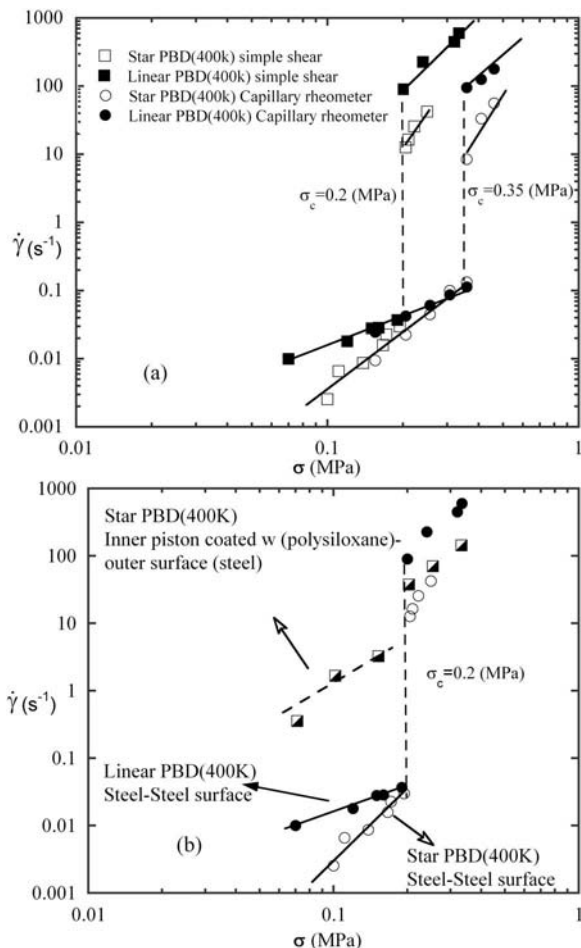


FIG. 9. (a) Flow curves of linear and four-arm star PBD at $T=25$ °C, where the gap is around 0.2 mm in simple shear flow; and in capillary rheometer, the die diameter $D=1.0$ mm, with the aspect ratio $L/D=15$. (b) Flow curves of linear and four-arm star PBD with bare and coated inner cylinder surfaces at $T=25$ °C, where the gap is 0.2 mm.

(2006)]. The preliminary results, shown in Fig. 10, convincingly indicate that the SST is an interfacial transition in shear flow of PIP. From the measured velocity profiles, the extrapolation length b , as depicted in Fig. 1(b), can be directly read from Fig. 10 to be around 0.9 mm, which agrees very well with b that can be calculated from Fig. 5 according to Eq. (2). A more systematic report using the PTV to study wall slip in both controlled-strain and controlled-force modes will be published in the future.

IV. CONCLUSION

In conclusion, using a specially designed constant-force piston shear rheometer, an interfacial SST has been characterized in simple shear of highly entangled polymer melts as a function molecular weight, chain architecture, and surface condition. The basic features are reminiscent of the earlier report [Yang *et al.* (1998)] of spurt-flow behavior in pressure-driven capillary flow rheometry. Since these melts undergo SST in simple shear, they must also suffer from the same consequences, i.e., spurt during capillary flow when

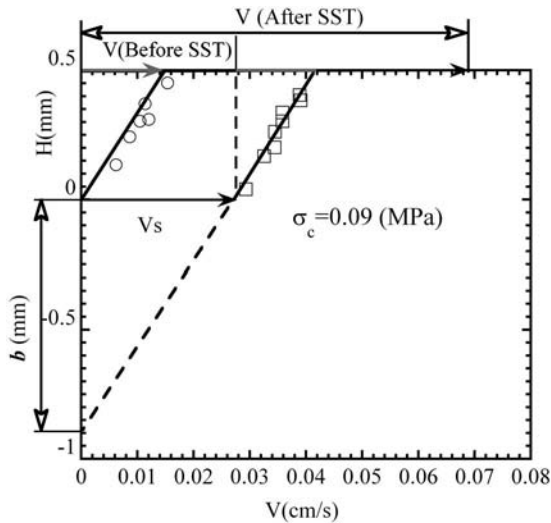


FIG. 10. Measurements using a PTV method applied to a sliding plate shear cell.

the applied pressure is high enough to produce a wall stress in excess of a critical value. One noticeable difference is that the critical shear stress σ_c for SST is distinctly lower in simple shear; around 0.2 MPa for PBD and 0.1 MPa for PIP. In both flow geometries, σ_c is independent of molecular weight and chain architecture.

ACKNOWLEDGMENT

This work was supported, in part, by an ACS-PRF grant (No. 40596-AC7) and by the National Science Foundation. One of the authors (P.E.B.) acknowledges receipt of a graduate assistantship from the University of Akron.

References

- Bagley, E. B., I. M. Cabot, and D. C. West, "Discontinuity in the flow curve of polyethylene," *J. Appl. Phys.* **29**, 109–110 (1958).
- Brochard, F., and P. G. de Gennes, "Shear-dependent slippage at a polymer/solid interface," *Langmuir* **8**, 3033–3037 (1992).
- Collyer, A. A., and D. W. Clegg, *Rheological Measurement* (Elsevier Applied Science, London, 1988), Chap. 12.
- Dao, T. T., and L. A. Archer, "Stick-slip dynamics of entangled polymer liquids," *Langmuir* **18**, 2616–2624 (2002).
- Denn, M. M., "Issues in viscoelastic fluid mechanics," *Annu. Rev. Fluid Mech.* **22**, 13–34 (1990).
- Doi, M., and S. F. Edwards, "Dynamics of concentrated polymer systems. Part 4. Rheological properties," *J. Chem. Soc., Faraday Trans. 2* **75**, 38–54 (1979).
- Durliat, E., H. Hervet, and L. Leger, "Influence of grafting density on wall slip of a polymer melt on a polymer brush," *Europhys. Lett.* **38**, 383–388 (1997).
- Fetters, L. J., D. J. Lohse, D. Richter, T. A. Witten, and A. Zirkel, "Connection between polymer molecular weight, density, chain dimensions and melt viscoelastic properties," *Macromolecules* **27**, 4639–4647 (1994).
- Koran, F., and J. M. Dealy, "A high pressure sliding plate rheometer for polymer melts," *J. Rheol.* **43**,

- 1279–1290 (1999a).
- Koran, F., and J. M. Dealy, “Wall slip of polyisobutylene: Interfacial and pressure effects,” *J. Rheol.* **43**, 1291–1306 (1999b).
- Laun, H. M., “Elastic properties of polyethylene melts at high shear rates with respect to extrusion,” *Rheol. Acta* **21**, 464–469 (1982).
- Leger, L., “Friction mechanisms and interfacial slip at fluid-solid interfaces,” *J. Phys.: Condens. Matter* **15**, S19–S29 (2003).
- Massey, G., H. Hervet, and L. Leger, “Investigation of the slip transition at the melt polymer interface,” *Europhys. Lett.* **43**, 83–88 (1998).
- McLeish, T. C. B., and R. C. Ball, “A molecular approach to the spurt effect in polymer melt flow,” *J. Polym. Sci., Part B: Polym. Phys.* **24**, 1735–1745 (1986).
- Mhetar, V. R., and L. A. Archer, “Slip in entangled polymer melts. 1. General features,” *Macromolecules* **31**, 8607–8616 (1998).
- Mhetar, V. R., and L. A. Archer, “Slip in entangled polymer melts. 2. Effect of surface treatment,” *Macromolecules* **31**, 8617–8622 (1998b).
- Migler, K. B., H. Hervet, and L. Leger, “Slip transition of a polymer melt under shear stress,” *Phys. Rev. Lett.* **70**, 287–290 (1993).
- Navier, C. L., *Mem. Acad. Sci. Inst. Fr.* **6**, 414 (1823).
- Pochettino, A., *Nuovo Cimento*, **8**, 77 (1914).
- Segel, M., *Phys. Z.*, **4**, 493 (1903).
- Smillo, F., “Wall slip and spurt of molten polymer,” M.S. thesis, McGill University, Montreal, Canada (2004).
- Stokes, G., “On the theories of the internal friction of fluids in motion, and of the equilibrium and motion of elastic solids,” *Trans. Cambridge Philos. Soc.* **8**, 287 (1845).
- Tapadia, P., and S. Q. Wang, “Nonlinear flow behavior of entangled polymer solutions: Yield like entanglement disentanglement transition,” *Macromolecules* **37**, 9083–9095 (2004).
- Tapadia, P., and S. Q. Wang, “Direct visualization of continuous simple shear in non-Newtonian polymeric fluids,” *Phys. Rev. Lett.* **96**, 016001 (2006).
- Tapadia, P., S. Ravindranath, and S. Q. Wang, “Banding in shear oscillation of entangled polymers,” *Phys. Rev. Lett.* **96**, 196001 (2006).
- Vinogradov, G. V., A. Y. Malkin, Y. G. Yanovskii, E. K. Borisenkova, B. V. Yarlykov, and G. V. Berezhnaya, “Viscoelastic properties and flow of narrow distribution polybutadienes and polyisoprenes,” *J. Polym. Sci., Polym. Phys. Ed.* **10**, 1061–1084 (1972).
- Wang, S. Q., and P. A. Drda, “Superfluid-like Stick-slip transition in capillary flow of linear polyethylene 1. General Features,” *Macromolecules* **29**, 2627–2632 (1996).
- Wang, S. Q., “Molecular transition and dynamics at polymer/wall interfaces: origins of flow instability and wall slip,” *Adv. Polym. Sci.* **138**, 227–275 (1999).
- Yang, X., S. Q. Wang, A. Halasa, and H. Ishida, “Fast flow behavior of highly entangled monodisperse polymers 1. Interfacial stick-slip transition of polybutadiene melts,” *Rheol. Acta* **37**, 415–423 (1998).

Copyright of Journal of Rheology is the property of Society of Rheology and its content may not be copied or emailed to multiple sites or posted to a listserv without the copyright holder's express written permission. However, users may print, download, or email articles for individual use.